

# Simultaneous Analysis System for Blood Pressure and Flow Using Photoplethysmography and Ultrasonic-Measurement-Integrated Simulation

Shusaku Sone, Toshiyuki Hayase, Kenichi Funamoto, Atsushi Shirai.

**Abstract**— We developed a simultaneous analysis system for blood pressure and flow using photoplethysmography and ultrasonic-measurement-integrated simulation. The validity of the system was confirmed by analysis of blood flow field in a carotid artery and corresponding wave intensity (WI) values.

## I. INTRODUCTION

The development and progression of cardiovascular diseases are closely related to hemodynamics. For advanced diagnosis of those diseases, it is necessary to understand the blood flow in detail. The authors have proposed and developed an ultrasonic-measurement-integrated (UMI) simulation to obtain information on hemodynamics such as blood flow and shear stress in the blood vessel [1]. This method employs unsteady computation with feedback of errors in Doppler velocities, velocity components in the ultrasound beam direction, between ultrasonic measurement and computation to make the numerical result converge to the actual blood flow field [2]. To date, we have constructed a two-dimensional UMI simulation system for clinical applications (Fig. 1) and shown the relationships between hemodynamic parameters based on calculated wall shear stress and pathology by investigating a number of clinical data of carotid arteries [3].

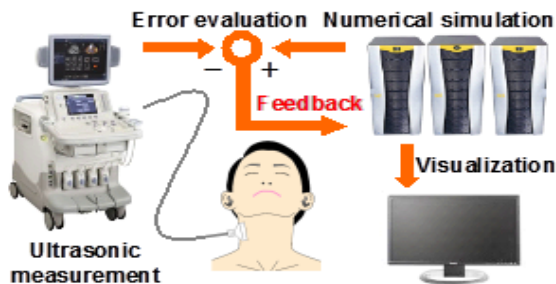


Figure 1. Ultrasonic-measurement-integrated simulation system

S. Sone is with the Graduate School of Biomedical Engineering, Tohoku University, 6-6-4 Aramaki Aza Aoba, Aoba-ku, Sendai 980-8579, JAPAN (phone:+81-22-217-5254 e-mail: sone@reynolds.ifs.tohoku.ac.jp).

T. Hayase is with the Institute of Fluid Science, Tohoku University, 2-1-1 Katahira, Aoba-ku, Sendai 980-8577, JAPAN (e-mail: hayase@ifs.tohoku.ac.jp).

K. Funamoto is with the Institute of Fluid Science, Tohoku University, 2-1-1 Katahira, Aoba-ku, Sendai 980-8577, JAPAN (e-mail: funamoto@reynolds.ifs.tohoku.ac.jp).

A. Shirai is with the Institute of Fluid Science, Tohoku University, 2-1-1 Katahira, Aoba-ku, Sendai 980-8577, JAPAN (e-mail: shirai@ifs.tohoku.ac.jp).

In the previous study, however, the reproduction of blood pressure was difficult since a blood vessel was treated as a rigid body. Study to reveal the mechanism of the development and progression of cardiovascular diseases should analyze blood pressure and flow simultaneously. Also, clinically, the wave intensity (WI) defined by the product of derivatives of blood pressure and blood velocity is of particular interest as an indicator of arteriosclerosis. Sugawara et al. reported a similarity relationship between a diameter and the pressure in the artery [4] and calculated WI [5] using pressure obtained from blood vessel diameter change measured from ultrasonic measurement and mean velocity obtained from ultrasonic Doppler measurement.

In the present study, a simultaneous analysis system for blood pressure and flow in a carotid artery was developed using photoplethysmography (Fig. 2) and UMI simulation. The validity of the system was confirmed by analysis of the blood flow field in a carotid artery and corresponding WI values.

## II. METHODS

### 2.1 Experimental procedure

The objective was the blood flow in a carotid artery of an informed healthy 23-year-old male volunteer. The experimental procedure is detailed below.

- 1) The volunteer's blood pressure was measured with a blood pressure meter device (HEM 9000AI, Omron Healthcare, JAPAN)
- 2) An ultrasound linear probe (10L, GE Helthcare Japan, JAPAN) was held by hand over the left common carotid artery and a photoplethysmographic sensor (infrared light 940 nm, personally developed) was held in place by adhesive tape.

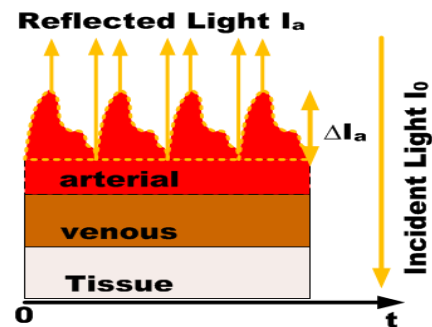


Figure 2. Photoplethysmography

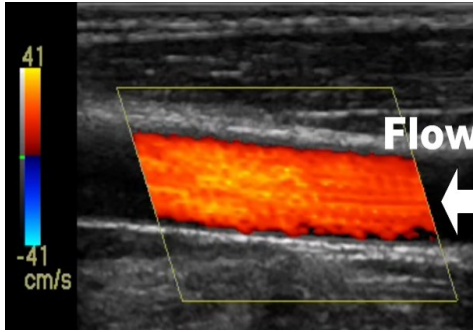


Figure 3. Color Doppler image of a carotid artery

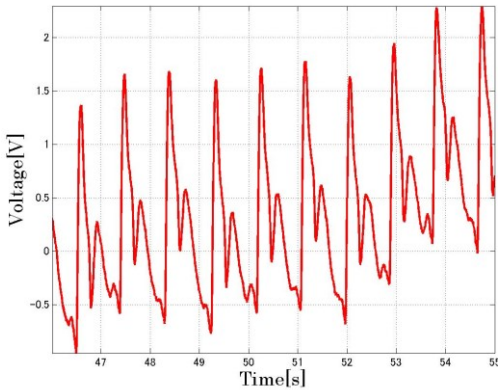


Figure 4. Pulse data obtained by photoplethysmographic sensor

Ultrasound color Doppler images for 5 cardiac cycles were acquired with an ultrasound diagnostic imaging device (LOGIQ7, GE Healthcare Japan, JAPAN) (Fig. 3). The center frequency and repetition frequency of ultrasound were 5 MHz and 5.4 kHz, respectively. Photoplethysmographic pulse data were simultaneously obtained with a photoplethysmographic sensor (Fig. 4). The measurements were repeated three times. 3) After the above measurements, the blood pressure was again measured.

## 2.2 Ultrasonic-Measurement-Integrated (UMI) Simulation

A brief explanation of UMI simulation is presented here. The governing equations of UMI simulation are the Navier-Stokes equation (1) and the pressure equation (2) for incompressible and viscous fluid flow,

$$\rho \left( \frac{\partial \mathbf{u}}{\partial t} + (\mathbf{u} \cdot \nabla) \mathbf{u} \right) = \mu \Delta \mathbf{u} - \nabla p + \mathbf{f} \quad (1)$$

$$\Delta p = -\rho \nabla \cdot (\mathbf{u} \cdot \nabla) \mathbf{u} + \nabla \cdot \mathbf{f} \quad (2)$$

where  $\mathbf{u}$  is the velocity vector,  $p$  is the pressure,  $t$  is time,  $\rho$  is the density,  $\mu$  is the dynamic viscosity, and  $\mathbf{f}$  is the feedback signal. It is defined as an artificial body force proportional to the difference of Doppler velocities,  $V$ , between the ultrasonic

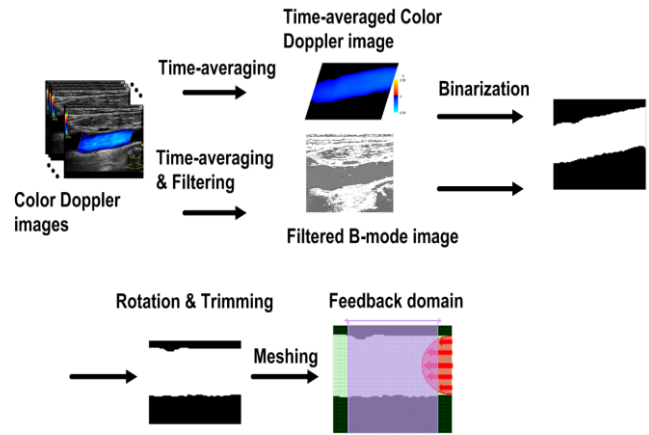


Figure 5. Method of computational grid generation

measurement and the numerical simulation as follows:

$$\mathbf{f} = -K_v^* \frac{V_c - V_m}{U} \left( \frac{\rho U^2}{L} \right) \quad (3)$$

where  $K_v^*$  is the feedback gain (non-dimensional),  $U$  is the characteristic velocity,  $L$  is the characteristic length, and subscripts  $m$  and  $c$  represent the ultrasonic measurement and UMI simulation, respectively. The special case with  $K_v^* = 0$  is the ordinary numerical simulation without feedback. Here, the measurement errors such as aliasing and lack of data are inherently included in the measured Doppler velocity,  $V_m$ . Hence, the present UMI simulation includes algorithms to detect measurement errors and to omit the feedback signals at the locations where the measurement errors were detected [6].

The above governing equations were discretized by means of the finite volume method and were solved with an algorithm similar to the SIMPLER method [7]. The analysis domain was a two-dimensional blood flow field in a cross section in a carotid artery including the blood vessel axis. The shape of the carotid artery was extracted by binarizing both the time-averaged color Doppler images and the time-averaged B-mode images. The shape was then rotated so that the main direction of the blood flow agreed with the  $x$ -directional axis, and a computational grid was generated (Fig. 5). The size of the computational grid is the same as the resolution of ultrasonic measurement, as  $\Delta x = 289 \mu\text{m}$  and  $\Delta y = 171 \mu\text{m}$ , respectively. Referring to the former study [8], the feedback domain was set from 1/8 to 7/8 of the computational domain in the axial direction. Feedback signals were added at each computational grid point in the feedback domain. Feedback gain was set to 0 (ordinary simulation) or to 100 (UMI simulation).

The blood flow rate was estimated to minimize the summation of absolute value of the error between the measured and computed Doppler velocities in the feedback domain by means of the golden section method [9]. Boundary conditions were a parabolic velocity profile in the upstream, free flow in the downstream, and no-slip on the wall.

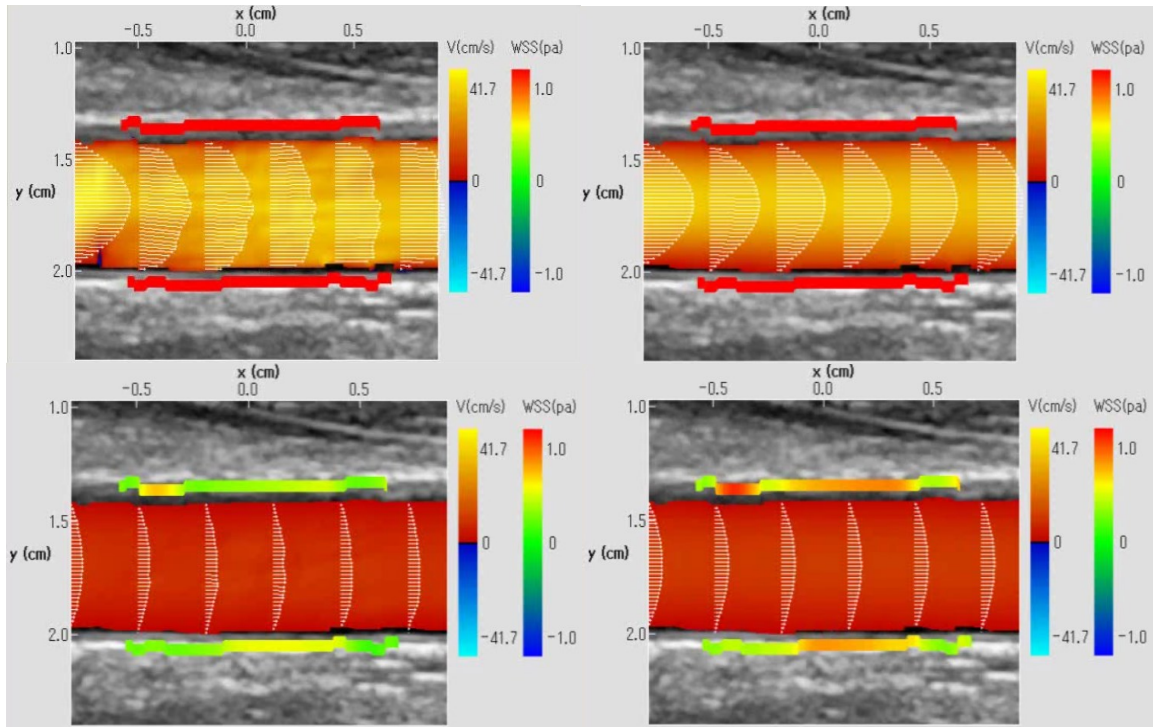


Figure 6. Blood flow distributions at systolic (top) and diastolic (bottom) phases by UMI simulation (left) and ordinary simulation (right)

### 2.3 Photoplethysmography

In Fig. 2, the Beer-Lambert principle gives the relationship between incident light strength  $I_0$  and reflected light strength  $I_a$  as,

$$\log \frac{I_a}{I_0} = -\mu_t L_t - \mu_v L_v - \mu_a L_a, \quad (4)$$

where  $\mu_t$ ,  $\mu_v$  and  $\mu_a$  are absorption of tissue, vein and artery, respectively, and  $L_t$ ,  $L_v$  and  $L_a$  are their thicknesses. Change of reflected light,  $\Delta I_a$ , of the arterial component according to systolic and diastolic blood pressure in Fig. 2 is shown in Fig. 4. Blood pressure waves were acquired from these data by calibrating systolic blood pressure value (113 mmHg) and diastolic blood pressure value (69 mmHg). We confirmed that those blood pressure waves agreed with those acquired from blood vessel wall movement using ultrasonic M mode data.

### 2.4 Wave Intensity (WI)

Wave intensity (WI) is defined as follows:

$$WI = \left( \frac{dP}{dt} \right) \left( \frac{dU}{dt} \right), \quad (5)$$

where  $P$  and  $U$  are the pressure and the flow velocity at an arbitrary point in a blood vessel. As WI changes according to the heart contractility, the vasodilating property and the load (state of the blood circulatory system), WI is a barometer of circulatory dynamics with much potential for analysis of the interface between cardiac ventricular and arterial systems [5][10].

## III. RESULTS AND DISCUSSION

Fig. 6 represents the results of the analysis of UMI and ordinary simulations for the blood flow field in a carotid artery. In the UMI simulation, the velocity profile converges to a complicated distribution in the downstream direction. On the other hand, the velocity profile of the ordinary simulation has an almost parabolic distribution in the downstream direction. The error between the UMI simulation and the actual Doppler velocity value was found to be almost half that of the ordinary simulation, indicating better accuracy in reproducing the blood flow [2].

Waveforms of the mean velocity and the pressure about 5 cardiac cycles are shown in Figs. 7 and 8, respectively. The mean velocity waveform in Fig. 7 was acquired by the ordinary simulation and UMI simulation. Little difference can be observed between them. The calibrated blood pressure waveform in Fig. 8 was derived from Fig. 4. Waveforms of the velocity and the pressure are almost periodic in these figures.

The representative waveforms of the pressure and the mean velocity in Figs. 7 and 8 as well as their derivatives are shown in Fig. 9. Since the waveform of the mean inlet velocity has low time resolution (15 Hz), that of the derivative becomes step-like shape. In addition, the second peak S2([12][13]) following the maximum velocity in systole may not be clearly measured.

Fig. 10 shows the time variation of WI acquired from values in Fig. 9. WI in a carotid artery shows typical first and second peaks similar to those shown in previous studies [5][10]. For better evaluation of WI parameter, the improvement of the time resolution of ultrasonic measurement is necessary.

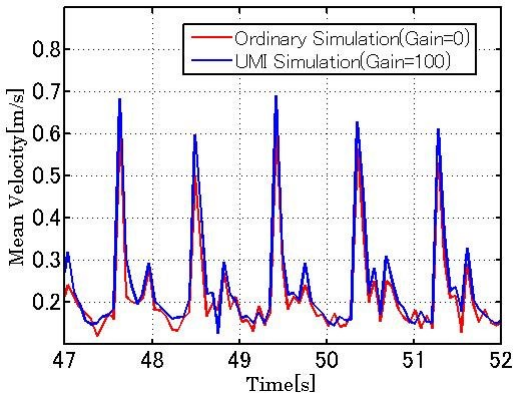


Figure 7. Mean velocity estimated by UMI and ordinary simulations with Doppler measurement

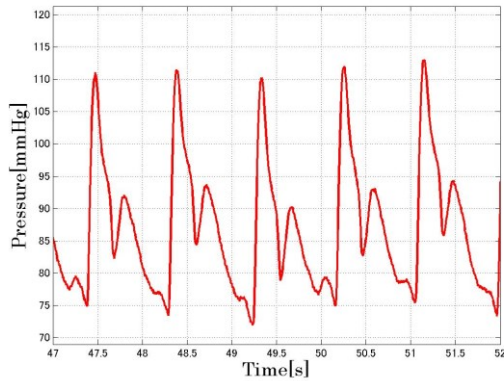


Figure 8. Blood pressure wave estimated by photoplethysmography and systolic and diastolic blood pressure measurement

#### IV. CONCLUSION

In this study, we developed a simultaneous analysis system for blood pressure and flow using photoplethysmography and UMI simulation. The validity of the system was confirmed by analysis of the blood flow field in a carotid artery and corresponding WI values.

#### REFERENCES

- [1] K. Funamoto et al., "Fundamental Study of Ultrasonic-Measurement-Integrated Simulation of Real Blood Flow in the Aorta," *Ann. Biomed. Eng.*, Vol. 33, pp. 415-428, 2005.
- [2] S. Sone et al., "Comparison between Ultrasonic-Measurement-Integrated Simulation and Ordinary Simulation with Measured Upstream Velocity Condition," *Proc. 8th Int. Conf. on Flow-Dynamics*, pp. 456-457, 2011.
- [3] T. Kato et al., "Evaluation of Wall Shear Stress on Carotid Artery with Ultrasonic-Measurement-Integrated Simulation," *Proc. 7th Int. Conf. on Flow-Dynamics*, pp. 542-543, 2010.
- [4] M. Sugawara et al., "Relationship between the Pressure and Diameter of the Carotid Artery in Humans," *Heart Vessels*, Vol. 15, pp. 49-51, 2000.
- [5] N. Ohte et al., "Clinical Usefulness of Carotid Arterial Wave Intensity in Assessing Left Ventricular Systolic and Early Diastolic Performance," *Heart Vessels*, Vol. 18, pp. 107-111, 2003.
- [6] K. Funamoto et al., "Numerical Analysis of Effects of Measurement Errors on Ultrasonic-Measurement-Integrated Simulation," *IEEE Trans. Biomed. Eng.*, Vol. 58, pp. 653-663, 2011.

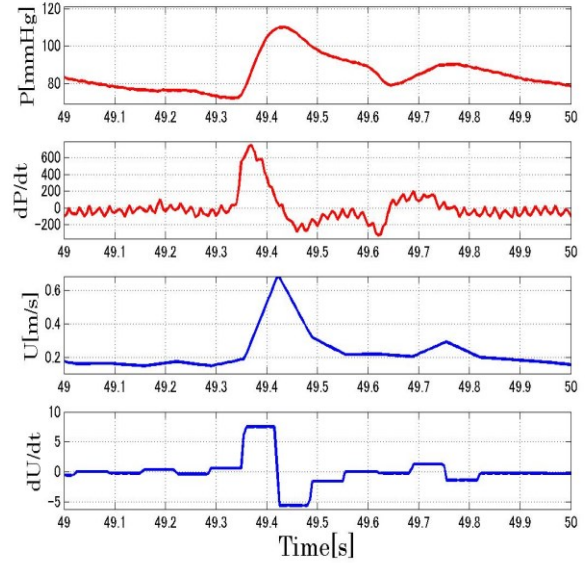


Figure 9. Pressure, the mean inlet velocity and their derivatives

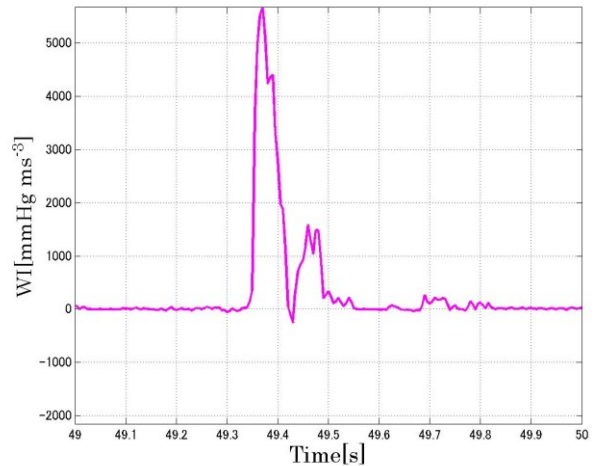


Figure 10. Time variation of WI

- [7] T. Hayase et al., "A Consistently Formulated QUICK Scheme for Fast and Stable Convergence Using Finite-Volume Iterative Calculation Procedures," *J. Comp. Physics*, Vol. 98, pp. 108-118, 1992.
- [8] K. Funamoto et al., "Numerical Study on Variation of Feedback Methods in Ultrasonic-Measurement-Integrated Simulation of Blood Flow in the Aneurysmal Aorta," *JSME Int. J., Ser. C*, Vol. 49, No. 1, pp. 144-155, 2006.
- [9] T. Yamagata et al., "Blood Flow Analysis by Ultrasonic-Measurement-Integrated Simulation with Flow Rate Estimation," *Proc. 9th Int. Symp. of Tohoku University Global COE Program Global Nano Biomed. Eng. Education and Research Network Centre*, pp. 114-115, 2009.
- [10] M. Sugawara et al., "Clinical Usefulness of Wave Intensity Analysis," *Med. Bio. Eng. Comp.*, Vol. 47, pp. 197-206, 2009.
- [11] A. Azhim et al., "Exercise Improved Age-Associated Changes in the Carotid Blood Velocity Waveforms," *J. Biomed. Pharm. Eng.*, pp. 17-26, 2007.
- [12] K. Hirata et al., "Age-Related Changes in Carotid Artery Flow and Pressure Pulses: Possible Implications for Cerebral Microvascular Disease," *Stroke*, Vol. 37, pp. 2552-2556, 2006.